

Article

Effect of Molecular Structure of C₁₀ Hydrocarbons on Production of Light Olefins in Catalytic Cracking

Lingyin Du, Yueyang Han and Youhao Xu *

Research Institute of Petroleum Processing, Sinopec, Xueyuan Road No. 18, Beijing 100083, China

* Correspondence: xuyouhao.ripp@sinopec.com

Abstract: The effect of the molecular structure of feedstock on the cracking reaction of C₁₀ hydrocarbons to ethylene and propylene over H-ZSM-5 zeolite was investigated. To better compare the effect of decane on the production of light olefins, the thermal cracking and catalytic cracking performance of decane were first investigated. As a comparison, the thermal cracking and catalytic cracking of decane were studied by cracking over quartz sand and H-ZSM-5. Compared with the thermal cracking reaction over quartz sand, the catalytic cracking reaction of decane over H-ZSM-5 has a significantly higher conversion and light olefins selectivity, especially when the reaction temperature was lower than 600 °C. On this basis, the catalytic cracking reactions of decane and decene over H-ZSM-5 were further compared. It was found that decene with a double bond structure had high reactivity over H-ZSM-5 and was almost completely converted, and the product was mainly olefin. Compared with decane as feedstock, it has a lower methane yield and higher selectivity of light olefins. Therefore, decene was more suitable for the production of light olefins than decane. To this end, we designed a new light olefin production process. Through olefin cracking, the yield of light olefins in the product can be effectively improved, and the proportion of different light olefins such as ethylene, propylene and butene can be flexibly adjusted.

Keywords: decane; decene; catalytic cracking; light olefins; molecular structure



Citation: Du, L.; Han, Y.; Xu, Y. Effect of Molecular Structure of C₁₀ Hydrocarbons on Production of Light Olefins in Catalytic Cracking. *Catalysts* **2023**, *13*, 1013. <https://doi.org/10.3390/catal13061013>

Academic Editors: Lei Liu and Zhijun Zuo

Received: 29 May 2023

Revised: 14 June 2023

Accepted: 14 June 2023

Published: 16 June 2023



Copyright: © 2023 by the authors. Licensee MDPI, Basel, Switzerland. This article is an open access article distributed under the terms and conditions of the Creative Commons Attribution (CC BY) license (<https://creativecommons.org/licenses/by/4.0/>).

1. Introduction

Ethylene and propylene were important basic raw materials in the petrochemical industry, which can be used to produce a variety of organic intermediates. Polyethylene, styrene, polypropylene, propylene oxide and many other products and intermediates can be produced by ethylene and propylene [1–3]. Steam cracking and fluid catalytic cracking (FCC) were two important processes for industrial production of light olefins [4–6]. However, the products obtained by the two processes were different. Among them, the products of the steam cracking unit have higher ethylene content, and the FCC process can obtain more propylene. Steam cracking requires high temperature, high energy consumption and high requirements for reactor materials [7]. Compared with the steam cracking process, the FCC process has low reaction temperature and low energy consumption. How to produce ethylene by FCC has attracted the attention of researchers [8–12].

In traditional industrial production, whether steam cracking or FCC, alkanes were mostly used as raw materials for the production of light olefins. However, the alkane molecules were relatively stable and difficult to crack. To obtain more light olefin yields, the reaction temperature must be increased, but this will also produce a large amount of low-value methane, resulting in a waste of resources [5,13,14]. Compared with alkanes, olefins have higher reactivity. Therefore, our research group developed a catalytic cracking process for targeted cracking to light olefins (TCO) [15]. The reaction raw materials were replaced with olefins that were easier to crack. The selectivity and yield of light olefin products were further improved by olefin cracking.

Alkanes and olefins have certain differences in molecular structure. Due to the presence of double bonds in the molecule, olefins were more likely to generate carbenium ions

than alkanes, and the reactivity will be significantly higher than alkanes [16]. The catalytic cracking reaction of hydrocarbon molecules on molecular sieves produces a variety of substances, and the reaction network was very complex. There were many studies on the cracking mechanism of alkanes and olefins [17–22]. Corma et al. [23] studied the reaction effects of n-heptane, n-decane, n-dodecane and n-tetradecane on USY, β and ZSM-5. The effects of operating variables, chain length and catalyst structure on product selectivity were studied. Ishihara et al. [24] analyzed the reaction effect of C_{12} – C_{32} hydrocarbons on the mixed catalyst of kaolin, β zeolite and Y zeolite with a curie point pyrolyzer instrument. It was found that with the increase in the carbon number of raw materials, the conversion, the selectivity of gasoline fractions and the proportion of olefins and alkanes increased significantly. At the same time, Y zeolite will produce more isomeric hydrocarbons than β zeolite. Bastiani et al. [25] studied the reaction effect of olefins on FER zeolite. The reaction performance of FER, FER and ZSM-5 mixed zeolite as catalysts and n-hexane and high olefin content gasoline as raw materials was studied. Compared with ZSM-5 zeolite, FER zeolite has better selectivity of propylene and butene, and ZSM-5 zeolite has better selectivity of ethylene.

Previous studies have sought to provide light olefin yields from catalytic materials [26–29]. Compared with the catalyst modification method to improve the yield of light olefins, the process change was a more convenient method. In this paper, the effects of alkanes and olefins on the formation of light olefins were compared and analyzed, and finding a new pathway to increase the production of light olefins was attempted.

2. Results and Discussion

2.1. Physicochemical Characterization of Catalyst

2.1.1. Textural Properties of Catalyst

The textural properties, including the surface area and pore volume of H-ZSM-5, were analyzed by nitrogen adsorption. Table 1 shows the surface area and pore volume of H-ZSM-5. It can be seen that H-ZSM-5 was mainly a microporous structure with a small number of mesopores. The average pore size distribution of ZSM-5 obtained from desorption branch of isotherms is shown in Figure 1. Through the pore size distribution of ZSM-5, the most probable distribution peak belonging to the mesoporous structure was not found in the mesoporous distribution range. It shows that there is no mesoporous structure above, which is consistent with the data results in Table 1.

Table 1. Textural properties of H-ZSM-5.

Sample	Surface Area (m^2g^{-1})			Pore Volume (cm^3g^{-1})		
	S_{BET}	S_{micro}	S_{ext}	V_{total}	V_{micro}	V_{meso}
H-ZSM-5	379.74	370.35	9.39	0.18	0.16	0.02

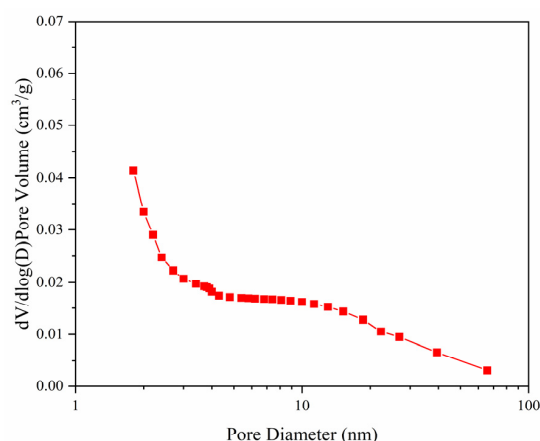


Figure 1. Average pore size distribution of ZSM-5 obtained from desorption branch of isotherms.

2.1.2. Catalysis Acidity

It was generally believed that the active center of the catalytic cracking reaction was the Brønsted acid site, so the analysis of acid properties was very important. The acid properties of the catalysts were analyzed by NH_3 -TPD and Py-IR methods, respectively, as shown in Figure 2. The Brønsted acid site and Lewis acid site were characterized by pyridine infrared spectroscopy, and quantitative analysis was carried out. As shown in Figure 2b, the characteristic peaks at the wavenumbers of 1550 cm^{-1} , 1455 cm^{-1} and 1490 cm^{-1} belonged to the peaks of pyridine adsorbed on Brønsted acid site, Lewis acid site and the result of the interaction of pyridine molecules at the of Brønsted acid site and Lewis acid site, respectively [30,31]. Pyridine desorption curves were recorded at 250 and 350 °C, respectively. The Brønsted acid site and Lewis acid site were estimated by the integral area of the peaks at different positions [26,32]. The results are shown in Table 2. It can be seen that the strong Brønsted acid sites of H-ZSM-5 after hydrothermal treatment were less than the weak Brønsted acid sites. Additionally, from the ratio of the Brønsted acid site and Lewis acid site, it can be seen that, compared with Lewis acid site, the Brønsted acid site was dominant in the strong acid site.

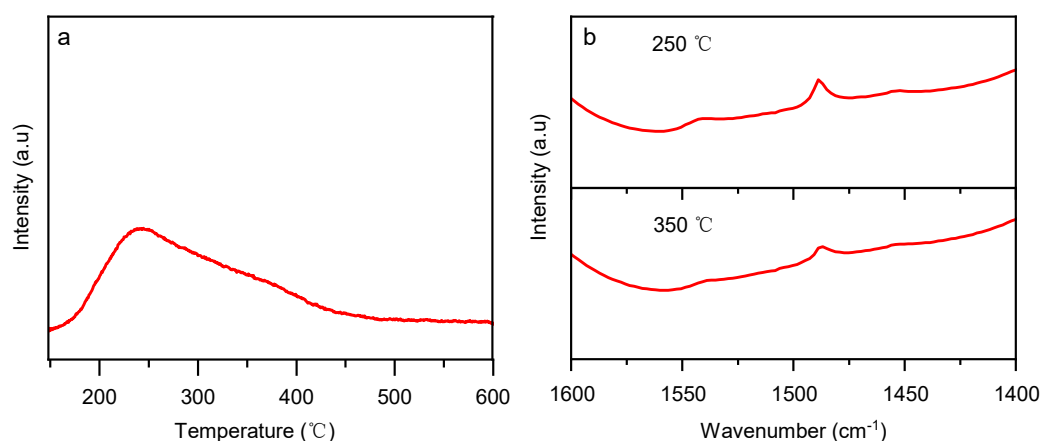


Figure 2. NH_3 -TPD (a) and Py-FTIR (b) spectra of H-ZSM-5.

Table 2. Acidity of H-ZSM-5 determined by Py-FTIR spectra.

Sample	B Acidity ($\mu\text{mol g}^{-1}$)		L Acidity ($\mu\text{mol g}^{-1}$)		Total Acidity ($\mu\text{mol g}^{-1}$)		B/L	
	250 °C	350 °C	250 °C	350 °C	250 °C	350 °C	250 °C	350 °C
H-ZSM-5	18.4	7.2	6.2	4.8	24.6	12.0	2.96	1.5

2.2. Thermal Cracking and Catalytic Cracking of Decane

Steam cracking and FCC process were two important processes for producing light olefins. Although both were processes for producing light olefins, there were great differences in the reaction mechanism between the two processes. Steam cracking follows the free radical reaction mechanism, and catalytic cracking reaction follows the carbocation reaction mechanism. To more specifically compare the difference between the two processes in the product, therefore, in this paper, quartz sand and H-ZSM-5 were used as catalysts to compare the thermal cracking reaction and the catalytic cracking reaction of decane. On the other hand, both the thermal cracking reaction and the catalytic cracking reaction were endothermic reactions, requiring a higher reaction temperature. Therefore, the effect of temperature on the cracking reaction was very important. In this paper, combined with the reaction conditions of steam cracking and catalytic cracking, the reaction temperature was set in the range of 500–750 °C.

The conversion and light olefin yields of the decane over quartz sand are shown in Figure 3a. It can be seen that the conversion of decane over quartz sand and the yield

of light olefins increase with the increase of reaction temperature. When the reaction temperature was lower than 600 °C, the conversion of decane over quartz sand was very low, and almost no thermal cracking reaction occurs. However, when the temperature exceeds 600 °C, the conversion and the yield of light olefins increase significantly faster. The highest conversion of 44.7% was obtained at 750 °C. The conversion of decane and the yield of light olefins over H-ZSM-5 are shown in Figure 3b. It can be seen that the conversion of decane and the yield of light olefins over H-ZSM-5 have the same trend as the reaction over quartz sand. The difference was that the conversion of decane over H-ZSM-5 was significantly higher than that over quartz sand when the temperature was lower than 600 °C because the catalyst reduces the activation energy of the reaction. However, when the temperature exceeds 600 °C, the gap between the two gradually decreases. At the reaction temperature of 750 °C, the conversion of decane over H-ZSM-5 reached the highest 53.74%.

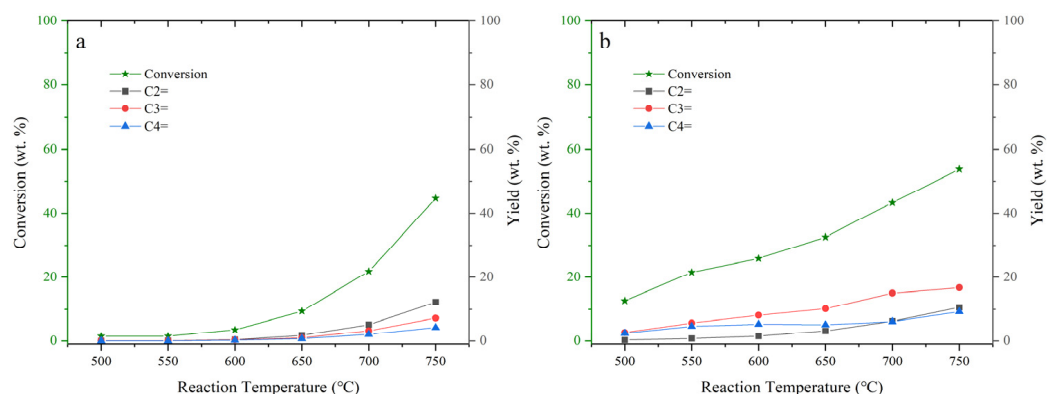


Figure 3. Conversion and light olefin yields of the decane cracking reaction vary with temperatures over quartz sand (a) and H-ZSM-5 (b), reaction conditions: catalyst 1.0 g; temperature, 500–750 °C; pressure, 0.1 MPa; feedstock flow rate, 2 mL min⁻¹; N₂ flow rate, 70 mL min⁻¹.

Olefin product yields of the decane cracking reaction vary with temperatures over quartz sand and H-ZSM-5 and are shown in Figure 4. It can be seen that the trend of olefin product yield over quartz sand and H-ZSM-5 was consistent, and the olefin product yield increased with the increase in reaction temperature. However, the yield of olefin products over quartz sand was significantly lower than that over H-ZSM-5. The reaction of decane over quartz sand produces more olefin products only after the reaction temperature reaches 700 °C. The olefin products were concentrated between C₂=–C₇=, especially C₂=. The olefin products of decane over H-ZSM-5 were mainly concentrated in C₂=–C₆= and more concentrated in the range of C₂=–C₄=. When the reaction temperature was lower than 600 °C, the yield of ethylene was low, and the products were mainly propylene and butylene. When the reaction temperature exceeds 600 °C, the ethylene content in the product begins to increase. The different distribution of olefin products in the products also reflects the different mechanisms of decane thermal cracking and catalytic cracking. The thermal cracking reaction occurs over the quartz sand, and the olefin product was mainly ethylene. The reaction over H-ZSM-5 was a catalytic cracking reaction, and the olefin product was mainly propylene butene.

Alkane product yields of the decane cracking reaction vary with temperatures over quartz sand and H-ZSM-5 and are shown in Figure 5. Since the feed is decane, we do not list the yield of decane. The alkane products of decane cracking over quartz sand were mainly methane and ethane, and the yield of alkane with high carbon number was very low. Different from the reaction products over quartz sand, the distribution of carbon number of the alkane products of decane over H-ZSM-5 was wide, mainly concentrated in C₁–C₇. This was because the thermal cracking reaction follows the free radical reaction mechanism, and the final products were mostly small molecules.

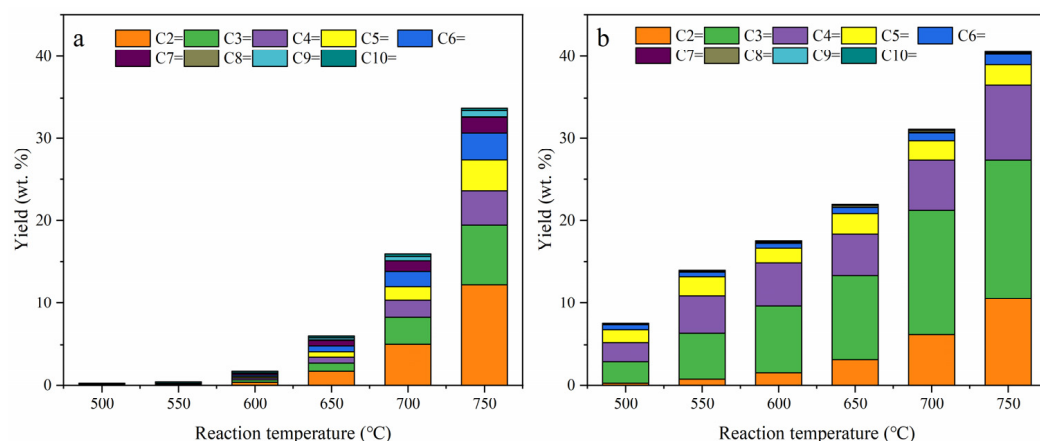


Figure 4. Olefin product yields of the decane cracking reaction vary with temperatures over quartz sand (a) and H-ZSM-5 (b), reaction conditions: catalyst 1.0 g; temperature, 500–750 °C; pressure, 0.1 MPa; feedstock flow rate, 2 mL min⁻¹; N₂ flow rate, 70 mL min⁻¹.

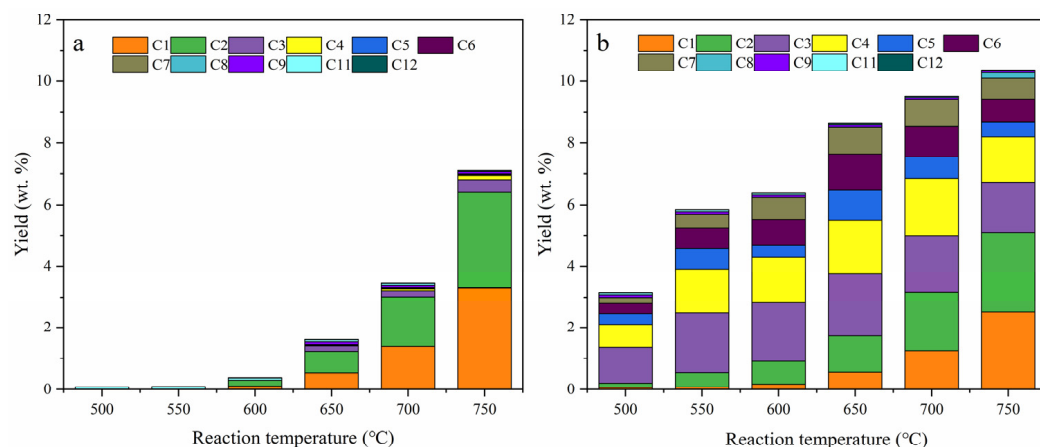


Figure 5. Alkane product yields of the decane cracking reaction vary with temperatures over quartz sand (a) and H-ZSM-5 (b), reaction conditions: catalyst 1.0 g; temperature, 500–750 °C; pressure, 0.1 MPa; feedstock flow rate, 2 mL min⁻¹; N₂ flow rate, 70 mL min⁻¹.

A methane molecule contains one carbon atom and four hydrogen atoms. Its chemical properties are relatively stable, and it is difficult to be used as a chemical raw material. Compared with ethylene and propylene, it is a low-value gas. So, we hope to produce as little methane gas as possible in the reaction. Additionally, we set two values of the molar ratio of ethylene to methane (E/M) and the molar ratio of propylene to methane (P/M) to evaluate the light olefin production plan. The E/M and P/M values of decane over quartz sand and H-ZSM-5 are shown in Figure 6. When the reaction temperature was lower than 600 °C, the methane yield was low, and the calculation value was inaccurate, so only four temperature points between 600 and 750 °C were calculated. It can be seen that in the case of quartz sand, the E/M and P/M values of decane thermal cracking do not change significantly with the increase in temperature. However, the E/M and P/M values of decane over H-ZSM-5 decreased significantly with the change of temperature, which may be due to the increase of methane growth rate with the increase of reaction temperature. When the reaction temperature reaches 750 °C, the E/M values of decane over quartz sand and H-ZSM-5 were 2.12 and 2.42, respectively, and the P/M values were 2.54 and 0.83, respectively. Compared with the thermal cracking reaction, the catalytic cracking reaction of decane produces less low-value methane while producing light olefins, which have a better atomic economy.

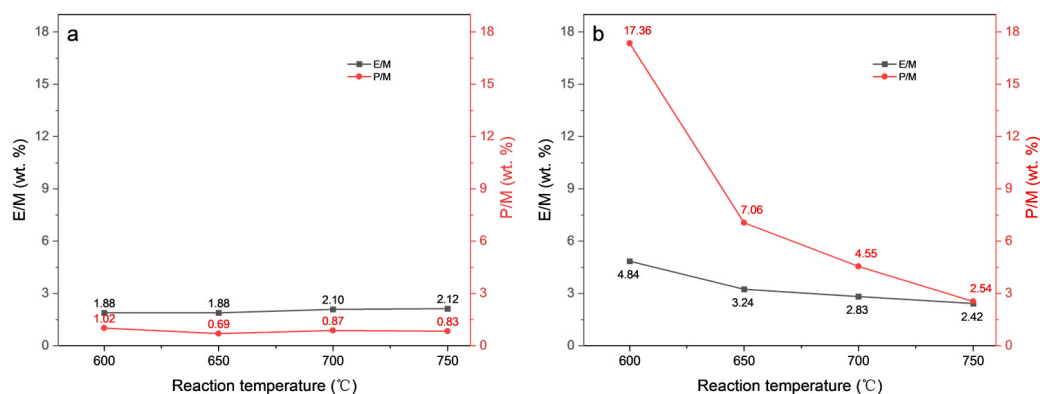


Figure 6. The value of E/M and P/M of decane over quartz sand (a) and H-ZSM-5 (b).

2.3. Catalytic Cracking of Decane and Decene

In the previous section, the difference between thermal cracking and catalytic cracking of decane was compared. By comparison, it was found that the atomic utilization rate of thermal cracking reaction was not high in the range of 500–750 °C. There were problems such as the low yield of light olefins and too many low-value products such as methane and ethane. Although the catalytic cracking reaction of decane will reduce the selectivity of methane to a certain extent, the yield of light olefins was not particularly high. For this reason, we chose the decene molecule with a double bond structure and decane for comparative experiments. The temperature range was also 500–750 °C.

The conversion of decane and decene and the yield of light olefins over H-ZSM-5 are shown in Figure 7. It can be seen that there was a clear difference in the conversion between the two. The highest conversion of decane reached 53.74% at 750 °C. Additionally, the conversion of decene remained high in all temperature ranges, almost completely converted. When decane was used as raw material, the yield of light olefins increases with the increase in temperature. When decene was used as raw material, the change trends of the three olefins were slightly different, and the yield of light olefins in the product was significantly higher than that when decane was used as raw material. This was due to the presence of double bonds, which greatly reduce the activation energy of the reaction and make the cracking reaction of decene easier.

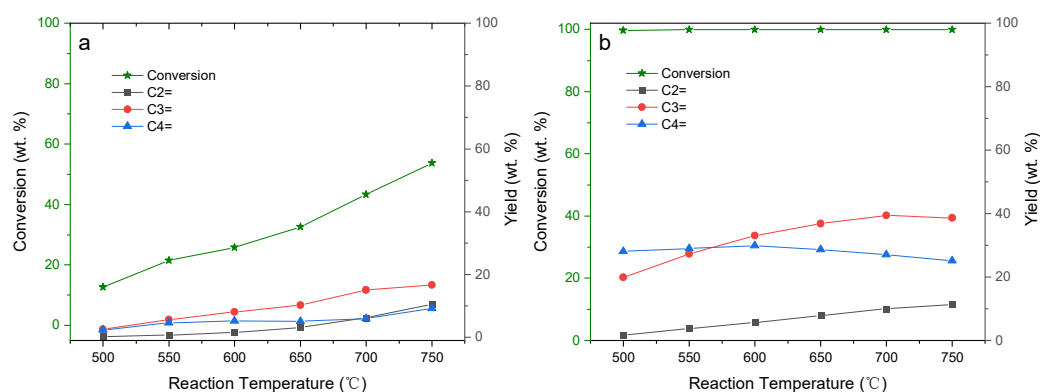


Figure 7. Reaction conversion and light olefin yield over H-ZSM-5 of decane (a) and decene (b), reaction conditions: catalyst 1.0 g; temperature, 500–750 °C; pressure, 0.1 MPa; feedstock flow rate, 2 mL min⁻¹; N₂ flow rate, 70 mL min⁻¹.

Olefin product yields over H-ZSM-5 of decane and decene are shown in Figure 8. It can be seen that there was a big difference between the two in the distribution of olefin products. The proportion of olefin products in the cracking products of decane was relatively low, even at 750 °C, the olefin products were only 40.52%, while the proportion of olefin products in the cracking products of decane was very high in all temperature ranges, basically above

80%. Additionally, the yield of olefin products with carbon atoms greater than four was more than that of decane as raw material.

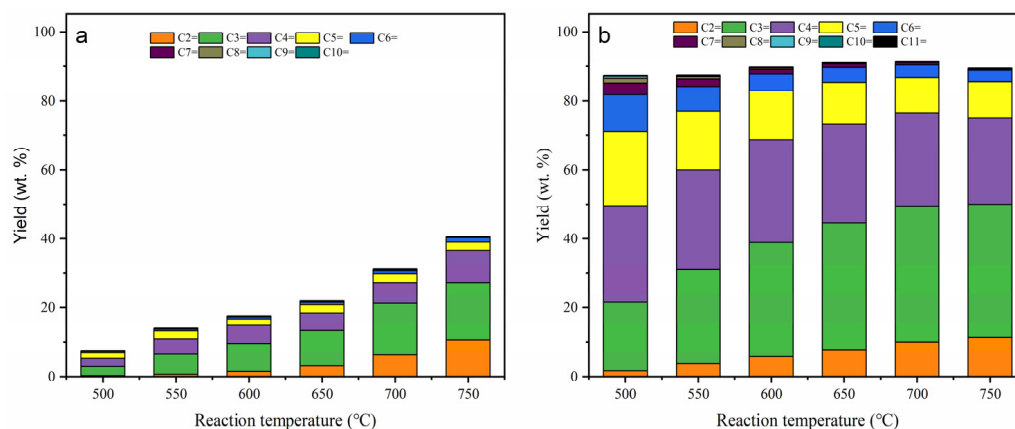


Figure 8. Olefin product yields over H-ZSM-5 of decane (a) and decene (b), reaction conditions: catalyst 1.0 g; temperature, 500–750 °C; pressure, 0.1 MPa; feedstock flow rate, 2 mL min⁻¹; N₂ flow rate, 70 mL min⁻¹.

Alkane product yields over H-ZSM-5 of decane and decene are shown in Figure 9. The alkane product distribution of decane and decene was also quite different. With the increase in temperature, the yield of alkanes in the pyrolysis products of decane was mainly concentrated in C₁–C₇. When decene was used as raw material, the proportion of alkanes in the products was relatively low, about 4%, and the difference in total alkanes content between different temperatures were not particularly large.

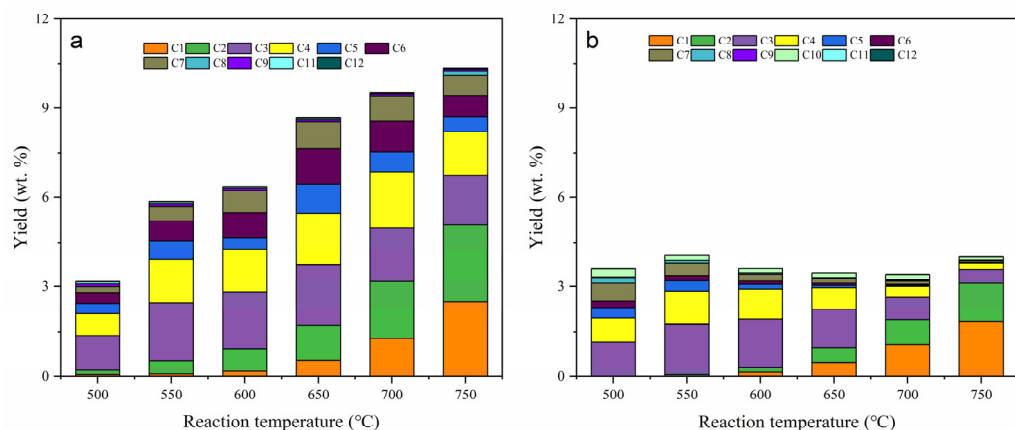


Figure 9. Alkane product yields over H-ZSM-5 of decane (a) and decene (b), reaction conditions: catalyst 1.0 g; temperature, 500–750 °C; pressure, 0.1 MPa; feedstock flow rate, 2 mL min⁻¹; N₂ flow rate, 70 mL min⁻¹.

The value of E/M and P/M of decane and decene over H-ZSM-5 is shown in Figure 10. Similarly, when the temperature was lower than 600 °C, methane was almost not generated, so only four temperature points of 600–750 °C were calculated. It can be seen that the changing trend of the two with the reaction temperature was consistent, and both decreased with the increase of the reaction temperature. The E/M and P/M values of decene products were higher than those of decane products, especially the P/M value. It can be seen that at the reaction temperature of 750 °C, the E/M values of decane and decene over H-ZSM-5 were 2.42 and 3.53, and the P/M values were 2.54 and 8.02, respectively. It shows that decene produces less low-value methane while producing light olefins. The yield of ethylene and propylene in decane was also higher than that of decane. Therefore, decene was more suitable for the production of light olefins than decane.

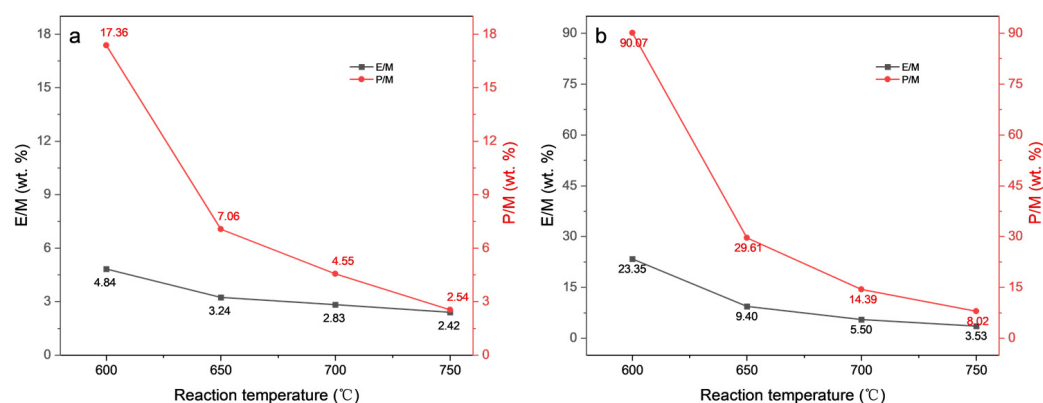
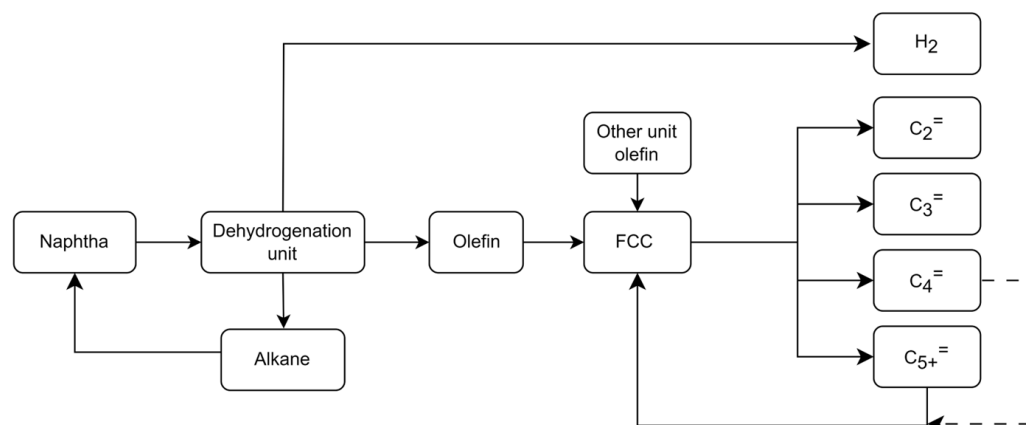


Figure 10. The value of E/M and P/M of decane (a) and decene (b) over H-ZSM-5.

2.4. Light Olefin Production Scheme

With the increase of electric vehicles, fossil fuel consumption continues to decrease. Traditional refineries that mainly produce fuel oil have begun to transform to produce chemical raw materials such as light olefins [33,34]. Steam cracking was an important process for the traditional production of light olefins, but it has problems such as high energy consumption, resulting in a waste of resources. In this paper, the steam cracking process was simulated by the thermal cracking of decane over quartz sand, and the three reactions of decane thermal cracking, decane catalytic cracking and decene catalytic cracking were compared. By comparing the three different reactions, it can be seen that the production of light olefins by decene catalytic cracking has higher E/M and P/M values, and the amount of low-value methane produced while producing light olefins was less. To this end, we designed a new efficient light olefin production process.

Different from the traditional production of light olefins using alkanes as raw materials, this scheme uses olefin cracking to produce light olefins. The simple process was shown in Scheme 1. First, the naphtha component passes through the dehydrogenation unit, and the generated hydrogen can be used as a product out of the device, and the incompletely dehydrogenated alkanes continue to enter the dehydrogenation unit for dehydrogenation. The dehydrogenated olefins enter the FCC unit, and the long-chain olefins were cracked to obtain light olefins. The incompletely cracked C_5^+ olefins continue to return to FCC for further cracking. If you need butene, butene can be used as a product directly out of the device. Or you can continue to return to the cracking unit for cracking, maximizing the production of ethylene and propylene. This scheme can flexibly adjust the proportion of ethylene, propylene and butylene in the product according to the market demand.



Scheme 1. Light olefin production scheme.

3. Experimental Section

3.1. Materials

H-ZSM-5 zeolite was provided by the 22nd Research Laboratory of Sinopec Research Institute of Petroleum Processing. After drying, the zeolite was pressed, crushed and sieved, and 20–40 mesh zeolite particles were screened. The treated particles were hydrothermally aged at 800 °C for 4 h. Decane (99%) and 1-decene (96%, the rest are olefin isomers) were purchased from Alfa Aesar.

3.2. Catalytic Cracking Experiment

The evaluation experiment was carried out in the fixed bed reactor in the laboratory. The reactor is a quartz reaction tube with an inner diameter of 6 mm. The catalyst (1 g, 20–40 mesh) was loaded into the quartz tube reactor, and the catalyst bed was cushioned with quartz cotton to prevent the catalyst from slipping. Before the experiment, the air tightness of the device was checked. After waiting for the catalyst bed to reach the predetermined temperature and stabilize, feed (1.7 g) was injected into the reactor through a syringe pump. The feed time was 70 s. After preheating and vaporization at the upper part of the reactor, the feed was driven by nitrogen to pass through the catalyst bed. After the feeding, the catalyst was purged with nitrogen for 900 s. High-temperature gas products were separated into gas products and liquid products by cooling (−19 °C). The liquid product was retained in the liquid receiving bottle and weighed after the reaction was completed. The volume of the cracking gas product was measured by the drainage method. After the reaction was completed, the reactor was heated to the regeneration temperature and coked with air for 600 s. The flue gas produced by coke burning was converted into CO₂ by a CO converter. The content of CO₂ in the flue gas was measured by an online CO₂ infrared analyzer, and the coke quality was calculated by integral. The composition of gaseous products was analyzed by an Agilent 7890A gas chromatograph (Agilent J&W HP-PLOT Al₂O₃ KCl column), and the composition of liquid products was analyzed by Agilent 7890A (Agilent J&W HP-PONA column). The conversion and yield were calculated as shown in Equations (1) and (2).

$$\text{Conversion} = \left(1 - \frac{\text{feed mass in the product}}{\text{feed mass}}\right) \times 100\%. \quad (1)$$

$$\text{Yield (C}_x\text{H}_y) = \frac{\text{C}_x\text{H}_y \text{ mass}}{\text{feed mass}} \times 100\% \quad (2)$$

where C_xH_y was the hydrocarbon in the product.

3.3. Catalysts Characterization

The pore structure properties (specific surface area, pore volume, etc.) of the samples were determined by N₂ adsorption–desorption experiments (Micromeritics, ASAP 2420). Firstly, 0.1 g catalyst was loaded into the sample tube. Then, the samples were degassed at 300 °C and 0.133 Pa for 4 h, and the adsorption isotherms were collected at −196 °C. The specific surface area of the sample was calculated by the Brunauer–Emmett–Teller (BET) method. The pore volume was calculated by the adsorption amount when the relative pressure of the adsorption branch was 0.98, and the pore size distribution was determined by the Barret–Joyner–Hallender (BJH) method based on the desorption branch in the adsorption isotherm.

The acid strength distribution of the catalyst was determined by NH₃ temperature-programmed desorption (NH₃-TPD), and the test instrument was Auto-ChemII2920 (Micromeritics). First, a 0.2 g (20–40 mesh) sample was placed in a U-shape quartz tube reactor. Helium was used as the carrier gas (25 mL/min), and the temperature was increased to 550 °C at a rate of 20 °C/min. After 60 min of purge, the temperature was reduced to 150 °C, and the temperature was kept constant for 5 min. It was switched to NH₃ adsorption for 60 min and then continued to purge with helium for 120 min until the baseline was stable. The desorption was carried out at a heating rate of 10 °C/min to 550 °C and kept

for 30 min. A TCD detector was used to detect the change in gas composition, and the total acid content was obtained by automatic integration of the instrument.

Brønsted and Lewis acid sites of zeolite were characterized through Fourier transform infrared spectroscopy of pyridine adsorption experiments (Nicolet 6700). The catalyst sample was ground into powder, and about 20 mg of the sample was weighed to make a self-supporting wafer, and the wafer was placed in an in situ cell equipped. The sample was treated at 500 °C and 1.33×10^{-3} Pa for 2 h. Then, the temperature dropped to 20 °C, and the saturated vapor of pyridine was adsorbed for 20 min. After the adsorption was completed, the program was heated to 250 °C vacua for desorption for 30 min. The temperature was raised to 350 °C vacua for desorption for 30 min to record and save the data.

4. Conclusions

The decane thermal cracking reaction and catalytic cracking reaction were compared over quartz sand and H-ZSM-5. It was observed that the conversion of thermal cracking and catalytic cracking of decane increased gradually with the increase in temperature. However, the difference was that when the reaction temperature exceeds 600 °C, the decane begins to undergo an obvious thermal cracking reaction, reaching the highest values of 44.7% and 53.74% at 750 °C. The conversion of the decane catalytic cracking reaction and the yield of light olefins were higher than that of the thermal cracking reaction. There was a big difference in the carbon number distribution of alkane products between the two. The thermal cracking reaction of decane was dominated by small molecules of methane and ethane. The carbon number distribution of alkane in the decane catalytic cracking reaction was wide, mainly concentrated in C₁–C₇. The E/M and P/M values of catalytic cracking reaction were higher than those of thermal cracking reaction, especially the P/M value.

Compared with decane catalytic cracking, the conversion of decene cracking was much higher. Even at 500 °C, the conversion of decene was still greater than 99%. At the same time, the yield of light olefins in the cracking products of decene was significantly higher. The calculated values of E/M and P/M of decene were significantly higher than those of decane cracking. Decene produces less low-value methane gas while producing light olefins. By comprehensive comparison of decane thermal cracking, decane catalytic cracking and decene catalytic cracking, it was found that decene catalytic cracking can obtain higher yield and selectivity of light olefins. It shows that olefin was a high-quality raw material for cracking to produce light olefins. To this end, we propose a new light olefin production scheme. Through the combination of alkane dehydrogenation technology and catalytic cracking technology, better light olefin production was achieved. At the same time, the scheme also has certain operational flexibility. Ethylene, propylene and butylene production can be regulated according to the market.

Author Contributions: Conceptualization, Y.X. and L.D.; methodology, Y.X.; software, Y.H.; validation, L.D., Y.H. and Y.X.; formal analysis, Y.H.; investigation, L.D.; resources, L.D.; data curation, L.D.; writing—original draft preparation, L.D.; writing—review and editing, Y.H.; visualization, Y.H.; supervision, Y.X.; project administration, Y.X.; funding acquisition, Y.X. All authors have read and agreed to the published version of the manuscript.

Funding: This work has been financially supported by research grant from the National Key R&D Program of China (No. 2021YFA1501204) and the China Petroleum & Chemical Corporation (Sinopec Corp.), China (Fund No. ST22001).

Data Availability Statement: Not applicable.

Conflicts of Interest: The authors declare no conflict of interest.

References

1. Blay, V.; Epelde, E.; Miravalles, R.; Perea, L.A. Converting olefins to propene: Ethene to propene and olefin cracking. *Catal. Rev.* **2018**, *60*, 278–335. [[CrossRef](#)]
2. Corma, A.; Corresa, E.; Mathieu, Y.; Sauvanaud, L.; Al-Bogami, S.; Al-Ghrami, M.S.; Bourane, A. Crude oil to chemicals: Light olefins from crude oil. *Catal. Sci. Technol.* **2017**, *7*, 12–46. [[CrossRef](#)]

3. Chernyak, S.A.; Corda, M.; Dath, J.-P.; Ordonsky, V.V.; Khodakov, A.Y. Light olefin synthesis from a diversity of renewable and fossil feedstocks: State-of-the-art and outlook. *Chem. Soc. Rev.* **2022**, *51*, 7994–8044. [[CrossRef](#)] [[PubMed](#)]
4. Gao, Y.; Neal, L.; Ding, D.; Wu, W.; Baroi, C.; Gaffney, A.M.; Li, F. Recent Advances in Intensified Ethylene Production—A Review. *ACS Catal.* **2019**, *9*, 8592–8621. [[CrossRef](#)]
5. Sadrameli, S.M. Thermal/catalytic cracking of hydrocarbons for the production of olefins: A state-of-the-art review I: Thermal cracking review. *Fuel* **2015**, *140*, 102–115. [[CrossRef](#)]
6. Sadrameli, S.M. Thermal/catalytic cracking of liquid hydrocarbons for the production of olefins: A state-of-the-art review II: Catalytic cracking review. *Fuel* **2016**, *173*, 285–297. [[CrossRef](#)]
7. Young, B.; Hawkins, T.R.; Chiquelin, C.; Sun, P.; Gracida-Alvarez, U.R.; Elgowainy, A. Environmental life cycle assessment of olefins and by-product hydrogen from steam cracking of natural gas liquids, naphtha, and gas oil. *J. Clean. Prod.* **2022**, *359*, 131884. [[CrossRef](#)]
8. Li, J.; Li, T.; Ma, H.; Sun, Q.; Li, C.; Ying, W.; Fang, D. Kinetics of coupling cracking of butene and pentene on modified HZSM-5 catalyst. *Chem. Eng. J.* **2018**, *346*, 397–405. [[CrossRef](#)]
9. Guo, Y.-H.; Pu, M.; Wu, J.-Y.; Zhang, J.-Y.; Chen, B.-H. Theoretical study of the cracking mechanisms of linear α -olefins catalyzed by zeolites. *Appl. Surf. Sci.* **2007**, *254*, 604–609. [[CrossRef](#)]
10. Dong, X.; Cheng, J.; Liu, C.; Wang, L. Mechanistic insight into the catalytic cracking mechanism of α -olefin on H-Y zeolite: A DFT study. *Comput. Theor. Chem.* **2021**, *1198*, 113183. [[CrossRef](#)]
11. Hao, J.; Cheng, D.-g.; Chen, F.; Zhan, X. n-Heptane catalytic cracking on ZSM-5 zeolite nanosheets: Effect of nanosheet thickness. *Microporous Mesoporous Mater.* **2021**, *310*, 110647. [[CrossRef](#)]
12. Corma, A.; Mengual, J.; Miguel, P.J. Stabilization of ZSM-5 zeolite catalysts for steam catalytic cracking of naphtha for production of propene and ethene. *Appl. Catal. A Gen.* **2012**, *421–422*, 121–134. [[CrossRef](#)]
13. Hou, X.; Ni, N.; Wang, Y.; Zhu, W.; Qiu, Y.; Diao, Z.; Liu, G.; Zhang, X. Roles of the free radical and carbenium ion mechanisms in pentane cracking to produce light olefins. *J. Anal. Appl. Pyrolysis* **2019**, *138*, 270–280. [[CrossRef](#)]
14. Ren, T.; Patel, M.; Blok, K. Olefins from conventional and heavy feedstocks: Energy use in steam cracking and alternative processes. *Energy* **2006**, *31*, 425–451. [[CrossRef](#)]
15. Xu, Y.; Zuo, Y.; Bai, X.; Du, L.; Han, Y. Development Background, Development Idea and Conceptual Design of FCC Process for Targeted Cracking to Light Olefins. *Pet. Process. Petrochem.* **2021**, *52*, 1–11.
16. Kissin, Y.V. Chemical Mechanisms of Catalytic Cracking over Solid Acidic Catalysts: Alkanes and Alkenes. *Catal. Rev.* **2001**, *43*, 85–146. [[CrossRef](#)]
17. Chen, C.-J.; Rangarajan, S.; Hill, I.M.; Bhan, A. Kinetics and Thermochemistry of C4–C6 Olefin Cracking on H-ZSM-5. *ACS Catal.* **2014**, *4*, 2319–2327. [[CrossRef](#)]
18. Standl, S.; Kühlewind, T.; Tonigold, M.; Hinrichsen, O. On Reaction Pathways and Intermediates During Catalytic Olefin Cracking over ZSM-5. *Ind. Eng. Chem. Res.* **2019**, *58*, 18107–18124. [[CrossRef](#)]
19. Blay, V.; Louis, B.; Miravalles, R.; Yokoi, T.; Peccatiello, K.A.; Clough, M.; Yilmaz, B. Engineering Zeolites for Catalytic Cracking to Light Olefins. *ACS Catal.* **2017**, *7*, 6542–6566. [[CrossRef](#)]
20. del Campo, P.; Navarro, M.T.; Shaikh, S.K.; Khokhar, M.D.; Aljumah, F.; Martínez, C.; Corma, A. Propene Production by Butene Cracking. Descriptors for Zeolite Catalysts. *ACS Catal.* **2020**, *10*, 11878–11891. [[CrossRef](#)]
21. Zhao, R.; Haller, G.L.; Lercher, J.A. Alkene adsorption and cracking on acidic zeolites—A gradual process of understanding. *Microporous Mesoporous Mater.* **2022**, *358*, 112390. [[CrossRef](#)]
22. He, M.; Ali, M.-F.; Song, Y.-Q.; Zhou, X.-L.; Wang, J.A.; Nie, X.-Y.; Wang, Z. Study on the deactivation mechanism of HZSM-5 in the process of catalytic cracking of n-hexane. *Chem. Eng. J.* **2023**, *451*, 138793. [[CrossRef](#)]
23. Corma, A.; Miguel, P.J.; Orchillés, A.V. Product selectivity effects during cracking of alkanes at very short and longer times on stream. *Appl. Catal. A: Gen.* **1996**, *138*, 57–73. [[CrossRef](#)]
24. Ishihara, A.; Ninomiya, M.; Hashimoto, T.; Nasu, H. Catalytic cracking of C12–C32 hydrocarbons by hierarchical β - and Y-zeolite-containing mesoporous silica and silica-alumina using Curie point pyrolyzer. *J. Anal. Appl. Pyrolysis* **2020**, *150*, 104876. [[CrossRef](#)]
25. Bastiani, R.; Lam, Y.L.; Henriques, C.A.; Teixeira da Silva, V. Application of ferrierite zeolite in high-olefin catalytic cracking. *Fuel* **2013**, *107*, 680–687. [[CrossRef](#)]
26. Lin, L.F.; Zhao, S.F.; Zhang, D.W.; Fan, H.; Liu, Y.M.; He, M.Y. Acid Strength Controlled Reaction Pathways for the Catalytic Cracking of 1-Pentene to Propene over ZSM-5. *ACS Catal.* **2015**, *5*, 4048–4059. [[CrossRef](#)]
27. Lin, L.; Qiu, C.; Zhuo, Z.; Zhang, D.; Zhao, S.; Wu, H.; Liu, Y.; He, M. Acid strength controlled reaction pathways for the catalytic cracking of 1-butene to propene over ZSM-5. *J. Catal.* **2014**, *309*, 136–145. [[CrossRef](#)]
28. Arudra, P.; Bhuiyan, T.I.; Akhtar, M.N.; Aitani, A.M.; Al-Khattaf, S.S.; Hattori, H. Silicalite-1 As Efficient Catalyst for Production of Propene from 1-Butene. *ACS Catal.* **2014**, *4*, 4205–4214. [[CrossRef](#)]
29. Lv, J.; Hua, Z.; Ge, T.; Zhou, J.; Zhou, J.; Liu, Z.; Guo, H.; Shi, J. Phosphorus modified hierarchically structured ZSM-5 zeolites for enhanced hydrothermal stability and intensified propylene production from 1-butene cracking. *Microporous Mesoporous Mater.* **2017**, *247*, 31–37. [[CrossRef](#)]
30. Fan, J.; Xiao, C.; Mei, J.; Liu, C.; Duan, A.; Li, J.; Liu, J.; Zhang, M. A hierarchical ZSM-22/PHTS composite material and its hydro-isomerization performance in hydro-upgrading of gasoline. *Catal. Sci. Technol.* **2021**, *11*, 5448–5459. [[CrossRef](#)]

31. Vitale, G.; Molero, H.; Hernandez, E.; Aquino, S.; Birss, V.; Pereira-Almao, P. One-pot preparation and characterization of bifunctional Ni-containing ZSM-5 catalysts. *Appl. Catal. A Gen.* **2013**, *452*, 75–87. [[CrossRef](#)]
32. Sun, H.; Cao, L.; Zhang, Y.; Zhao, L.; Gao, J.; Xu, C. Effect of Catalyst Acidity and Reaction Temperature on Hexene Cracking Reaction to Produce Propylene. *Energy Fuels* **2021**, *35*, 3295–3306. [[CrossRef](#)]
33. Jermy, B.R.; Tanimu, A.; Siddiqui, M.A.; Qureshi, Z.S.; Aitani, A.; Akah, A.; Xu, Q.; AlHerz, M. Crude oil conversion to chemicals over green synthesized ZSM-5 zeolite. *Fuel Process. Technol.* **2023**, *241*, 107610. [[CrossRef](#)]
34. Alabdullah, M.; Rodriguez-Gomez, A.; Shoinkhorova, T.; Dikhtiarenko, A.; Chowdhury, A.D.; Hita, I.; Kulkarni, S.R.; Vittenet, J.; Sarathy, S.M.; Castaño, P. One-step conversion of crude oil to light olefins using a multi-zone reactor. *Nat. Catal.* **2021**, *4*, 233–241. [[CrossRef](#)]

Disclaimer/Publisher's Note: The statements, opinions and data contained in all publications are solely those of the individual author(s) and contributor(s) and not of MDPI and/or the editor(s). MDPI and/or the editor(s) disclaim responsibility for any injury to people or property resulting from any ideas, methods, instructions or products referred to in the content.